

NUMERICAL STUDY OF FROST-INDUCED RING FRACTURES IN CAST IRON WATER PIPES

Susan A. Trickey, MSc, GeoEngineering Centre at Queen's-RMC, Kingston, ON, K7L 3N6

Ian D. Moore, PhD, PEng (Professor), GeoEngineering Centre at Queen's-RMC, Kingston, ON, K7L 3N6

ABSTRACT

Three dimensional response of buried water pipes subject to differential frost movement is investigated using the finite element method. The mechanism of behaviour and the potential for ring fracture of these cast iron water pipes under variable frost conditions are explored. A pipe buried at the transition between a local road and an arterial is considered. While the arterial is constructed of high grade pavement, the local road used a lower grade pavement incorporating native, frost susceptible soil as the subbase. Initial investigations examine how frost and ice lens depth control the pipe deflection and moment. Secondary analyses examine the effects of pipe flexural stiffness and axial stiffness on peak deflection and moment. The investigation concludes with a study of the effect of pavement stiffness on pipe deflection and moment. Initial findings indicate that the pipe approaches failure when ice lens formation increases the volume of the overlying soil by 25%.

RÉSUMÉ

La réponse tridimensionnelle des conduits d'eau enterrées soumises au mouvement différentiel de gel est étudiée en utilisant la méthode des éléments finis. Le mécanisme du comportement et le potentiel pour la rupture d'anneau de ces conduites d'eau en fonte dans des conditions variables de gel sont explorés. Une conduite enterrée à la transition entre une route locale et une artère est construite avec une chaussée de qualité supérieure, la route locale a une chaussée de qualité inférieure, utilisant le sol natif, sensible au gel comme couche de fondation. Les études initiales ont examiné comment le gel et la profondeur des lentilles de glace contrôlent la flèche et le moment de la conduite. Les analyses secondaires examinent les effets de la rigidité à la flexion et axiale de la conduite la flèche et le moment maximaux. La recherche se termine avec une étude de l'effet de la rigidité de la chaussée sur la flèche et le moment de la conduite. Les résultats initiaux indiquent que la conduite approche la rupture quand la formation des lentilles de glace augmente le volume du sou-jacent de 25%

1. INTRODUCTION

Seasonal frost penetration is a concern in regions such as Ontario, Canada, where this frost penetration results in differential ground movements which can cause ring fracture in buried infrastructure such as cast iron water pipes. Extensive research has been funded by the resource industry on numerical analysis of chilled gas pipelines e.g. Nixon (1983) and Selvadurai (1993, 1999). Other researchers such as Rajani and Zhan (1996) and Rajani et al. (1996) have developed simplified methods of estimating axial frost loads on buried water pipes by employing Winkler spring models.

The authors report on a three dimensional finite element study of water pipes under differential ground movements. Preliminary analyses investigate three frost loading conditions of pore water freezing and ice lens formation and their impact on pipe deflection and moment. Secondary analyses assess the impact of varying problem geometry and material characteristics on pipe deflection, moment and potential for ring fracture under a standard, well defined differential frost loading condition as determined from the preliminary analysis. The results are outlined from these two

series of analyses for a cast iron water pipe located beneath a transition of pavements with different frost susceptibilities.

2. STATEMENT OF PROBLEM

2.1 Cast iron water pipe failure

Cast iron water pipe failure may result from a variety of mechanisms such as circumferential or ring fracture, longitudinal breaks, joint failure, blowouts, or corrosion pits (Rajani et al. 1996). The failure mechanism of particular interest for the present parametric study is ring fracture. The following study investigates cast iron water pipe ring fracture as a result of differential frost action, under varying frost loading conditions, model geometry and material conditions, to develop a better understanding of this failure mechanism and the longitudinal soil-pipe response.

2.2 Frost-related volume expansion

The two primary components of frost movement are incorporated into the analyses: isotropic pore water

expansion and orthotropic ice lens formation, Figure 1. The first component is associated with the 9% volume increase of soil pore water as it freezes, while the second component relates to water migration from the unfrozen soil to the freezing front where ice lenses form. A 25% volume increase is imposed to model ice lens formation which accounts for 20% of the final soil volume. This is half the high value reported by Konrad et al. (1995) for frost susceptible sensitive clays.

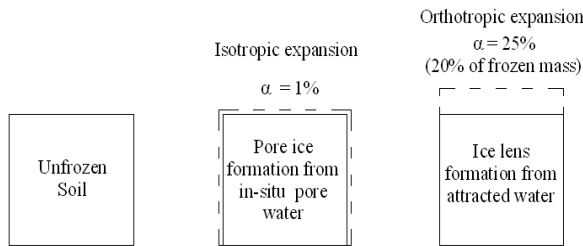


Fig. 1. Frost-related volume expansion

2.3 Nonuniform expansion at pavement transition

An intersection where a major arterial road joins a local residential street is investigated, Figure 2. The major arterial is constructed of high grade pavement materials with a non frost susceptible subbase, while the residential street is constructed of low grade pavement materials with a frost susceptible subbase. A cast iron water pipe is located in a trench backfilled with native frost susceptible material at a depth of 2 m below the surface. This is representative of common burial conditions for cast iron water pipes installed in the last 75 years. The pavement transition from frost susceptible subbase to non frost susceptible subbase material imposes a nonuniform ground response on the buried water pipe below, as a result of volumetric expansion in the frost susceptible subbase. The nonuniform ground movements cause pipe deflection and moments that may induce ring fracture.

2.4 Parameter selection

The road structure consists of a flexible pavement, with an asphaltic concrete top layer, a granular base, and a subbase. The subbase material is either constructed of frost susceptible or non frost susceptible material according to the pavement grade. Each pavement layer has an associated Young's modulus E and Poisson's ratio ν . Table 1 summarizes the material properties and layer depths used in the analysis. The pavement geometry is illustrated in Figure 2. Trickey and Moore (2005b) provide further discussion of the material properties and geometry of the reference case.

The native fine grained frost susceptible soil material is assume to be a linear elastic isotropic material with a constant unfrozen Young's modulus E_s and Poisson's ratio ν_s . The unfrozen soil modulus was selected to reflect the characteristics of a fine grained frost susceptible soil based on the data of Leroueil et al. (1991). Shear failure is not modeled, and there is no explicit consideration of the contact pressures between the pipe and soil (fully bonded interaction is modeled between pipe and structure, with no limits in the shear strength across the soil-pipe interface). The pavement structure lies above a foundation of frost susceptible native material. The trench backfill and local road subbase are constructed of the same frost susceptible soil. The frozen soil modulus E_f was selected based on the experimental findings of Yuanlin and Carbee (1983), who suggest a relationship for frozen soil modulus with respect to temperature change. The soil material properties for the reference case are summarized in Table 2.

Table 1. Pavement material and geometric properties

Material	Modulus (MPa)	Poisson's ratio	Depth (m)
Asphaltic Concrete	85,000	0.4	0.13
Granular Base	150	0.3	0.15
Subbase (Non Frost Susceptible)	125	0.3	0.45
Subbase (Frost Susceptible)	400	0.3	0.45

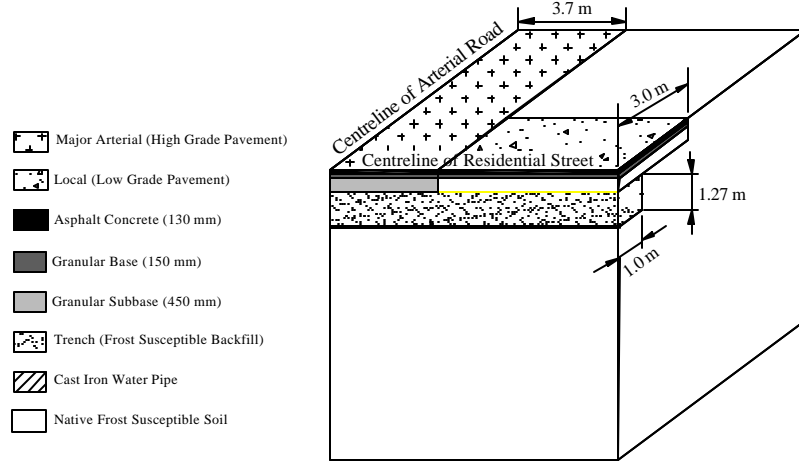


Fig. 2. Problem geometry

Table 2. Soil and water pipe material properties

Material	Modulus (MPa)	Poisson's ratio
Frost susceptible soil (Unfrozen)	3	0.3
Frost susceptible soil (Frozen)	400	0.3
Cast iron water pipe	75,000	0.0

A water pipe of diameter, d of 150 mm and wall thickness, t of 10 mm was selected for the reference analysis based on measurements taken from a City of Hamilton field specimen. The cast iron water pipe has an average Young's modulus E_p of 75 GPa. Pipe material properties are summarized in Table 2. The influence of these choices on the pipe response is investigated in the parametric study.

The flexural stiffness factor, K_r and axial stiffness factor, K are used to express the stiffness relative to the soil, of the cast iron water pipe. These stiffness factors are defined by Poulos (1974) and Poulos and Davis (1980), as follows:

$$[1] \quad K_r = \frac{E_p I}{E_s L^4}$$

$$[2] \quad K = \frac{E_p A}{E_s A_0}$$

where K_r = the relative flexural stiffness of the buried pipeline
 K = the relative axial stiffness of the buried pipe
 E_s = the modulus of elasticity of the soil (kPa)
 E_p = the modulus of elasticity of the pipe (kPa)
 I = the moment of inertia of the pipe (m^4)
 L = the length of the pipe (m)
 A = the cross sectional area of the pipe modeled as a prism (m^2)
 A_0 = the area bounded by the outer circumference of the pipe (m^2)

Factor K_r relates the flexural stiffness of the pipe with respect to the soil, while the axial stiffness factor, K relates the axial stiffness of the prismatic pipe relative to the soil it displaces. The larger the values of K_r and K , the stiffer the pipe is relative to the soil (Poulos 1974, Poulos & Davis 1980, Trickey and Moore 2005a).

The maximum deflections and moments of the cast iron water pipe are the principal outcomes of the study. The potential for ring fracture is also of interest, and will be assessed by comparing moments to the moment capacity of the pipe. Normalized ultimate moment for the grey cast iron pipe $M_u/E_p d^3 = 7.1 \times 10^{-5}$ is shown on various figures.

3. STATEMENT OF PROBLEM

3.1 Mesh design

The commercial finite element package ANSYS 7.1 was used to perform the three dimensional analyses. The problem modeled one of the four quarters of the

region about the centerline of the major arterial using linear elastic materials and tetrahedral elements. Figures 2 and 3 illustrate the mesh geometry and mesh design used for the study. Sensitivity analyses performed by Trickey and Moore (2005b) determined that a mesh width and depth of 10 m provides a reasonably efficient analysis. The vertical and base boundaries were modeled as smooth and rigid, preventing horizontal and vertical movements respectively. The top surface was left unrestrained. The pipe was modeled as a rectangular solid to simplify the analysis. Details regarding the determination of the pipe dimensions may be found in Trickey and Moore (2005b).

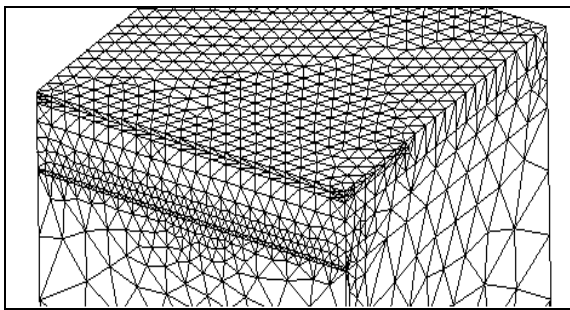


Fig. 3. Finite element mesh

3.2 Frost modeling

A coupled thermal-structural analysis was employed to model the effects of frost. A coupled analysis allows the results from one analysis to be applied as loads in another. Initially the model was constructed using thermal elements. A temperature change of 1°C was then applied to the frost heave zone and the thermal analysis performed. A secondary analysis was constructed using compatible solid elements and the results of the thermal analysis applied as body loads in the structural analysis.

Frost loading was modeled as a volumetric expansion which combined isotropic pore water freezing and orthotropic vertical ground heave due to ice lens formation. This expansion occurred in the frost susceptible material within the zone 2 m above the pipe. Thermal expansion coefficients, α_{il} and α_{pw} were assigned to the soil materials within this region to produce either orthotropic ice lens formation or isotropic pore water expansion associated with the temperature change. Table 3 outlines the thermal expansion coefficient α_{pw} selected to simulate a 9% pore volume increase associated with pore water freezing, and α_{il} selected to simulate a 25% increase in the soil volume associated with the formation of ice lenses. The 1°C temperature change is an arbitrary

value selected to impose the desired volume expansion. Any other temperature change could have been employed, provided that corresponding changes were made to the thermal expansion coefficients.

Table 3. Thermal expansion coefficients

Volume expansion	Thermal expansion coefficient (°C)
Isotropic (pore water freezing)	0.01
Orthotropic (ice lens formation)	0.25

4. PRELIMINARY ANALYSIS

Preliminary analyses investigated the impact of three different frost loading conditions on pipe deflection and moment, Figure 4. The first frost loading condition modeled isotropic pore water freezing in the frost susceptible subbase and trench backfill material to the 2 m burial depth of the pipe. The second frost condition combined orthotropic ice lens formation to a depth of 0.505 m below the surface in the frost susceptible materials and isotropic pore water freezing to the burial depth of the pipe. The final frost condition modeled ice lens formation to the depth of the frost susceptible subbase (0.73 m below the surface) and isotropic pore water freezing in the trench backfill material (2 m below the surface). Figure 4 illustrates the different frost loading conditions.

4.1 Deflections

Figure 5 plots normalized deflection profiles for the three different frost loading conditions. The pipe deflection mechanism is clearly illustrated in this figure. The pipe moves downward under the local frost susceptible road as it experiences the frost loading from pore water freezing or ice lens formation acting above it. The section of the pipe located beneath the non frost susceptible arterial road responds by moving upwards. A transition zone develops between the non frost susceptible material and the frost susceptible material where a point of inflexion develops in the pipe.

It is evident that frost conditions which incorporate ice lens formation yield deflections of an order of magnitude higher than those involving only pore water expansion. The depth of the pore water expansion or ice lens formation therefore influences peak pipe deflections.

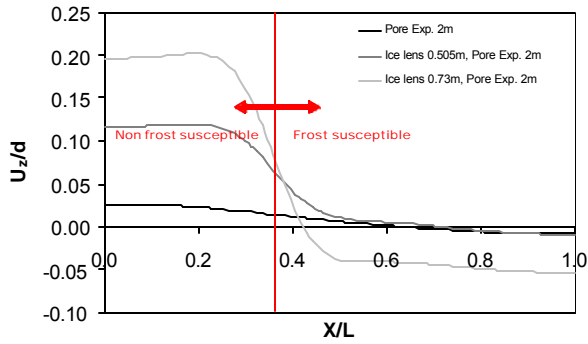


Fig. 5. Deflection profiles under various frost loading conditions

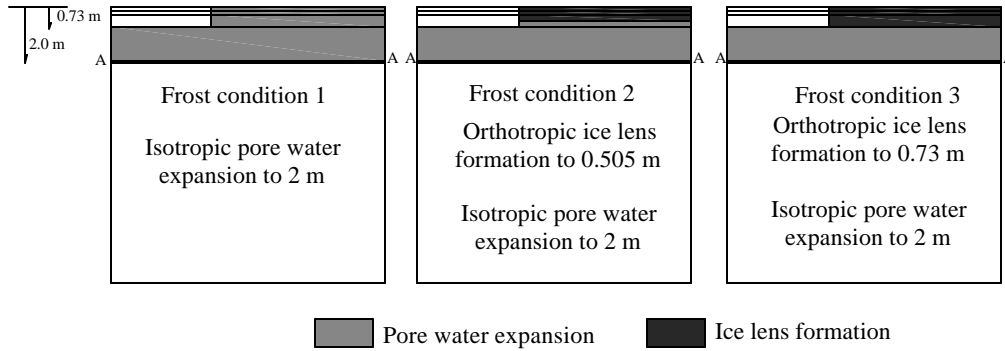


Fig. 4. Frost loading cases

4.2 Moments

Normalized moment profiles are shown in Figure 6 for the various frost loading conditions. The maximum pipe moments experienced by the pipe can be attributed to the regions of the deflection profiles in Figure 5 which have the greatest curvature. As with deflections, analyses which incorporated ice lens formation yield peak moments an order of magnitude greater than those due solely to pore water freezing. However, unlike deflections, pipe moments are a function of curvature and not the depth of pore water expansion or formation of ice lenses which results from the differential ground movements that occur in the overlying subbase material. Moments are calculated from curvatures; as differences in quantity of ice lensing above the pipe develop for the section of pipe under the frost-susceptible subbase relative to the pipe under the arterial road, the pipe curvature increases, and this increases pipe moments so that they approach the failure capacity of the grey cast iron. Further investigation into the effects of changes in the

problem geometry and material characteristics are warranted to establish the key factors influencing pipe fracture.

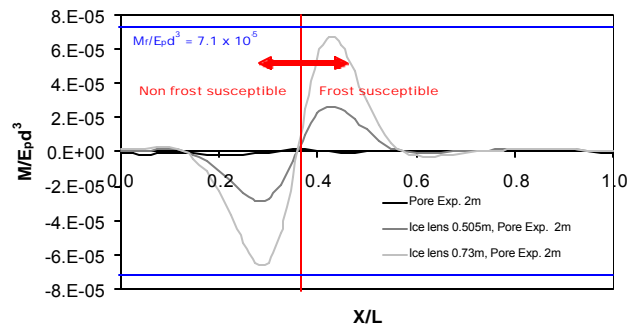


Fig. 6. Moment profiles under various frost loading conditions

5. PARAMETRIC STUDY

A parametric study was performed to examine the impact of changes in specific geometric and material parameters on the maximum pipe deflection, maximum moment, and the potential for ring fracture. A consistent loading case of orthotropic ice lens formation to a depth of 0.73 m and isotropic pore water expansion to a depth of 2 m was selected for the parametric study. This loading case is considered to be a reasonable buried pipe scenario. Changes in maximum pipe deflections and moments are examined as a result of different pipe and soil characteristics such as relative axial pipe stiffness, flexural pipe stiffness and pavement stiffness.

5.1 Effect of relative axial stiffness

The first case investigated the effects of relative axial pipe stiffness, K on pipe deflection and moment. Relative axial stiffness values of 4 times and $\frac{1}{4}$ of the original cast iron pipe relative axial stiffness were input into the model (equivalent to changing pipe modulus or wall thickness by that factor of 4). This was achieved while maintaining the same pipe flexural stiffness by changing the pipe dimensions. Results indicate that, as expected, changes in relative axial stiffness of the pipe had little effect on maximum pipe deflection and moment, provided the pipe's flexural stiffness is maintained unchanged. Figure 7 illustrates the normalized pipe deflections and moments. Decreases in the relative axial stiffness are seen to induce some additional uplift of the pipe under the arterial road, and small increases in peak bending moment (an increase of approximately 6% as relative axial stiffness is decreased by a factor of 4 below the reference case). While this does bring the moment even closer to the moment capacity, it generally appears that the moments and deflections are not very sensitive to changes in K . This lack of sensitivity is a function of the magnitude of the relative axial stiffness of the pipe. If the relative pipe axial stiffness is either very high as in the cases presented here or very low the effect of relative axial stiffness is negligible. Should the relative pipe stiffness fall within the transition zone between very stiff and very flexible, the effect on pipe deflection and moment would be significant.

5.2 Effect of soil modulus

A secondary study was performed to monitor the impact of changes in native soil modulus on the maximum pipe deflection and moment. The pipe's

relative flexural stiffness was changed by factors of 10, by adjusting the native soil modulus. The results of maximum normalized pipe deflection and moment are plotted in Figure 8. Maximum pipe uplift under the arterial road increased as native soil modulus decreased, though maximum normalized moment changed only slightly. Changes in uplift can be attributed to the decreases in soil stiffness, allowing the pipe to deflect more readily. The contrary occurs in the case of decreased relative flexural stiffness, since increases in soil modulus lead to greater resistance to pipe deflection. The moment trends indicate that as the soil modulus increases it provides more resistance to longitudinal curvature, decreasing the pipe moments. While it is also evident that the water pipe moves closer to flexural failure with decreasing relative flexural stiffness, the magnitude of the increase in normalized pipe moment is negligible.

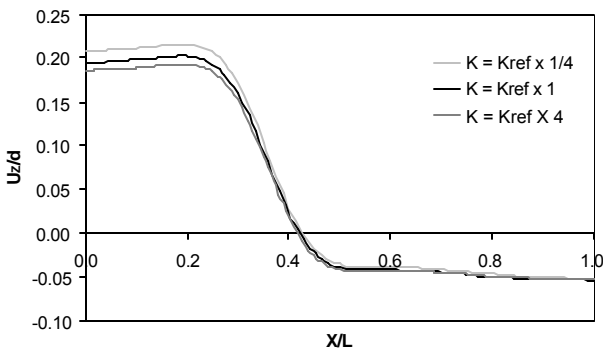
The native frost susceptible soil used for the reference analysis represents a weak soil with a modulus of 3 MPa where it is unfrozen (at greater depths than 2m). Differential pipe movement which results due to the nonuniformity of intersection subbase materials is also a function of the stiffness of that underlying soil material. A weak underlying material like that employed in the reference case allows the pipe to push farther down into the soil under the local road and greater uplift under the major arterial. Replacing the native soil material with a stiffer material reduces the differential pipe deflection as movements in the underlying strata are restrained. Low stiffness soil like that considered in the reference analysis may also allow the pipe to sink progressively lower with each subsequent freezing season, transitioning the soil from a normally consolidated material to a stiffer overconsolidated soil.

5.3 Effect of pavement stiffness

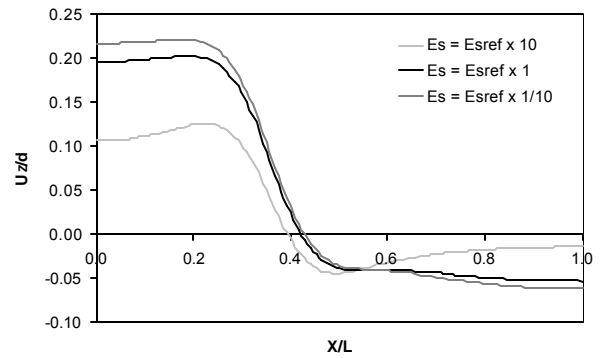
The third case investigated the impact of pavement stiffness on pipe deflection and moment. Three variations were imposed to monitor this effect. In each case, reductions in pavement layer modulus were examined, since these could occur if the pavement structure was poorly constructed. The first analysis featured a four fold decrease in the modulus of the asphaltic concrete layer. The results indicate that by decreasing the asphaltic concrete modulus, the downward deflections in the frost susceptible region slightly decreased, and the upward deflections in the non frost susceptible region also decreased. These changes decreased the pipe curvature and therefore the moments. The reduced asphaltic concrete modulus appears to reduce the impact of the differential frost heave on the pipe below, given the

reduction in vertical restraint to the volumetric expansion shown in Figure 9. The second analysis featured a four fold decrease in the modulus of the non frost susceptible granular base. Reducing that granular base modulus also decreased the relative pipe movements across the transition zone between the non frost susceptible and frost susceptible subbase materials. The final analysis used a

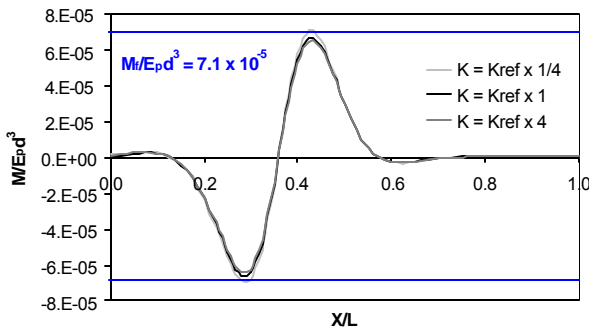
reduced modulus for the non frost susceptible subbase modulus. As with both of the other pavement stiffness reductions, decreases in the subbase modulus decreased pipe moment. In all cases these analyses indicate that a reduction in the stiffness of any of the pavement layers decreases the likelihood of pipe failure.



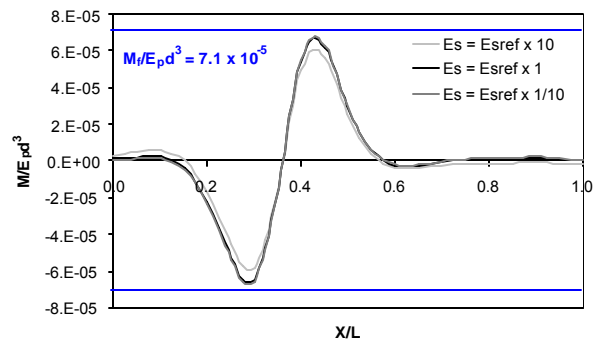
a. Deflections



a. Deflections



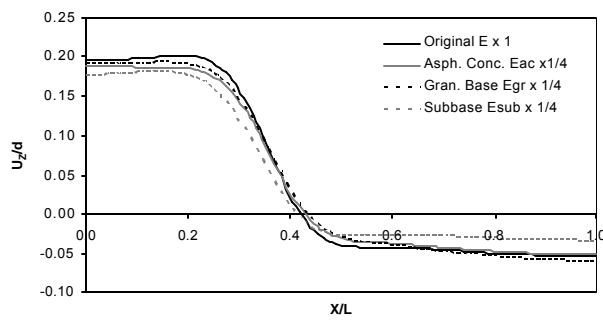
b. Moments



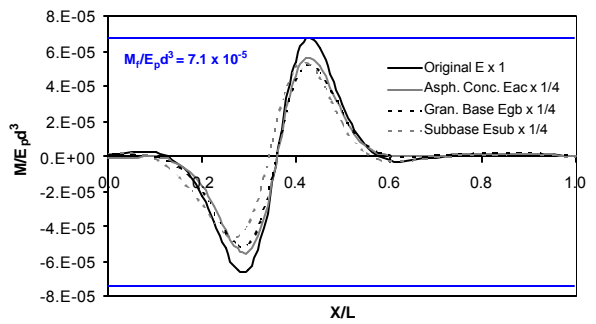
b. Moments

Fig. 7. Effects of relative axial stiffness, K

Fig. 8. Effects of soil modulus



a. Deflections



b. Moments

Fig. 9. Effects of pavement stiffness: moments

6. SUMMARY AND CONCLUSIONS

A three dimensional finite element study of the effects of differential frost movements on a buried cast iron water pipe located beneath a transition between pavements of different frost susceptibility was undertaken. Pipe deflection, moments and potential for ring fracture were investigated. Initial investigations examined three frost loading conditions considering the effects of both isotropic pore water expansion and orthotropic ice lens formation. Results indicated that analyses which incorporated the formation of ice lenses produced peak pipe deflections and moments an order of magnitude greater than those which simply analysed pore water expansion. However, the depth of either of these frost mechanisms influences the magnitude of pipe deflection. Moments which are a function of pipe curvature, are controlled by the differential frost movements which occur in the soil materials located above the pipe.

Secondary analyses investigate the impact of variable geometric and material conditions on the cast iron water pipe. The parametric study examined the effect of relative axial pipe stiffness, relative flexural pipe stiffness and pavement stiffness on pipe deflections, moments, and likelihood of failure due to ring fracture. Changes made to the relative axial stiffness of the pipe while maintaining the pipe's relative flexural stiffness had a small impact on pipe deflections and moments. Modifying soil modulus to impose an increase in relative pipe flexural stiffness resulted in increasing pipe deflections, but negligible change in moments. Decreases in pavement stiffness lead to decreases in moments, in turn reducing the potential for pipe failure. Further research is needed, where actual field data is compared to the material presented in this article, regarding the geometric and material conditions that effect pipe failure. Collaboration with municipalities to make field observations would provide a better overall understanding of the mechanisms of behaviour, which may be used to modify or calibrate future numerical models.

References

Konrad, J. -M., Bergeron, G., Roy, M., La Rochelle, P. and Leroueil, S. (1995) Field observations of frost action in intact and weathered Champlain Sea clay. *Canadian Geotechnical Journal*, 32:689-700.

Leroueil, S., Tardif, J., Roy, M., La Rochelle, P. & Konrad, J.-M. (1991) Effects of frost on the

mechanical behaviour of Champlain Sea clays. *Canadian Geotechnical Journal*, 28: 690-697.

Nixon, J. F., Morgenstern, N. R. & Ressor, S. N. (1983) Frost heave – pipeline interaction continuum mechanics. *Canadian Geotechnical Journal*, 20:251-261.

Poulos, H.G. (1974) Analysis of longitudinal behavior of buried pipes. *Conference on Analysis and Design in Geotechnical Engineering*, 9-12 June, Austin, Texas, ASCE. 1:189-223.

Poulos, H.G. & Davis, E.H. (1980) *Pile Foundation and Design*. New York, John Wiley & Sons, Inc.

Rajani, B. & Zhan, C. (1996) On estimation of frost loads. *Canadian Geotechnical Journal*, 33: 629-641.

Rajani, B., Zhan, C. & Kuraoka, S. (1996) Pipe-soil interaction analysis of jointed water mains. *Canadian Geotechnical Journal*, 33: 393-404.

Selvadurai, A. P. S., Hu, J. & Konuk, I. (1999) Computational modeling of frost heave induced soil-pipeline interaction II. Modeling of experiments at the Caen test facility. *Cold Regions Science and Technology*, 29: 229-257.

Selvadurai, A. P. S. & Shinde, S. B. (1993) Frost Heave Induced Mechanics of Buried Pipelines. *Journal of Geotechnical Engineering*, 119 (12): 1929-1951.

Trickey, S. A. & Moore, I. D. (2005a) Three dimensional response of buried pipes under circular surface loading. *Journal of Geotechnical and Geoenvironmental Engineering*, ASCE (to appear).

Trickey, S. A. & Moore, I. D. (2005b) Numerical Analysis of Frost-Induced Bending Moments in Cast Iron Water Pipes, *Computers and Geotechnics*, Submitted for publication, May 2005.

Yuanlin, Z. & Carbee, D. L. (1984) Uniaxial compressive strength of frozen silt under constant deformation rates. *Cold Regions Science and Technology*, 9: 3 -15.